intermediates to various enzyme partners. Structures of apo-, holo-, and saturated acyl-ACPs indicate that the acyl groups are housed inside a hydrophobic binding cavity between three largely parallel helices. Molecular dynamics (MD) simulations have previously been used to illustrate the behaviour of various saturated acyl chains attached to ACP, in excellent agreement with experimental data. However, relatively little is known about the fatty acyl derivatives formed during the elongation of the acyl chains, namely the β-ketoacyl-, β-hydroxyacyl-, and enoyl-intermediates. ACP is one of the most abundant proteins in *Escherichia coli* and possesses a large number of interacting enzymes. As such, we seek to understand how the enzymes of fatty acid biosynthesis recognize which derivative is bound by ACP. To address this, we conducted numerous MD simulations of *E. coli* ACP with β-ketoacyl-, β-hydroxyacyl-, and enoyl- intermediates. The unconstrained MD simulations were set up with the attachment either in a solvent exposed or a solvent shielded conformation inside the hydrophobic binding pocket of ACP. We investigate a range of acyl group derivatives attached to ACP spanning from four to eighteen carbon groups in length to develop our understanding of the differences imparted on ACP by various acyl chain lengths. The results of the simulations of fatty acyl derivatives will provide a first look at the manner in which ACP accommodates these binding groups. What these data contribute to the understanding of enzyme:ACP interactions and substrate recognition by fatty acid synthase enzymes will be discussed.

338-Pos Board B217

The Dependence Of Coiled-coil Chirality On Elastic Energy

Sara Sadeghi, Eldon Emberly.
Simon Fraser University, Burnaby, BC, Canada.

Coiled coils are proteins that consist of two or more alpha-helices that wrap around each other to form a super-helical structure. Using a continuum elastic model, a recent paper [1] has shown that the chirality of the super-helical twist is dictated by the chirality of the pattern of hydrophobic residues on each helix only when the bending and twisting energy of each helix is considered. In the absence of any energy cost due to the flexible motions of each helix, they showed that there is a family of structures which are consistent with the hydrophobic pattern. Using a coarse-grained atomistic model for coiled coils that includes the flexible degrees of freedom for each helix, we have carried out monte-carlo simulations to examine how the energy and chirality of coiled coils depends on the strength of the elastic energy. We find that there is an optimal weighting of the elastic energy that leads to the coiled coils adopting the same chirality as the hydrophobic pattern on each helix. We then explored how the chirality of the coiled coil changed under the application of an applied force or an applied torque. Our findings are compared to recent measurements on the mechanics of coiled-coils from single-molecule studies.

[1] S. Neukirch, A. Goriely and A.C. Hausrath, PRL, 100, 038105 (2008).

339-Pos Board B218

Computational Modeling of the Structural Mechanism Linking Ligand and Corepressor Binding to Thyroid Hormone Receptors

Yi Chen.
University of Michigan, Ann Arbor, MI, USA.

Thyroid hormone receptors (TRs) are nuclear receptors with two functional states. Upon binding to the thyroid hormone, TRs recruit coactivator proteins and activate gene transcription. Without the hormone ligands, TRs interact with corepressor proteins and repress transcription. Due to the importance of the thyroid hormone action in embryo development, metabolism, heart rhythm and cholesterol level, the molecular mechanism behind the functional switch has been studied extensively. However, the current available crystal structures of thyroid hormone receptor ligand binding domains (LBDs) are all in the ligand-bound (holo) form, with no revelation on ligand-free (apo) form or transcription corepressor bound form. In order to elucidate the complete apo to holo switch process, we constructed homology models of apo TR from the available apo structures of interrelated nuclear receptors: retinoid acid receptor (RXR) and peroxisome proliferators activated receptor (PPAR). Both models were subjected to energy minimization followed by molecular dynamic (MD) simulation. Analysis of the MD simulations proved that the model based on PPAR was more stable than the model based on RXR. As a result, unlike the prevailing idea that TRs would exert a major structural change in the C-terminal activation helix (AF2) domain upon ligand binding, TRs exhibit only subtle changes at the AF2 domain. Our model predicts that the recruitment of corepressor proteins, which require the relocation of the AF2 domain, is more appropriately portrayed as an induced fit process. Additionally, we constructed homology models of TR LBD in complex with the nuclear receptor interacting domains of corepressor proteins. Molecular dynamic simulation of this receptor-correpressor complex system in the absence or presence of the ligand thyroid hormone has identified correlated conformational changes that may be important for the functional switch.

340-Pos Board B219

Effects Of Reactive Oxygen Species On Cyan Fluorescent Protein

Luis Alvarez[1], Fabienne Merola[2], Chantal Houée-Levin[1], Filippo Rusconi[3], Marie Erard[1].
[1]Université Paris-Sud, Orsay, France, [2]Centre National de la Recherche Scientifique, CNRS, Orsay, France, [3]Muséum National d'Histoire Naturelle, Paris, France.

Recent advances in microscopy techniques and the development of many different colour variants of the GFP family of proteins allow for a more direct analysis of protein function in live cells. The advantage of genetically coded fluorescent protein probes is often offset by their photophysical properties which usually make them very sensitive to cellular environmental changes. Among these, reactive oxygen species (ROS) are an essential part of key cellular processes (mitochondria respiration, apoptosis) and are also involved in the pathogenesis of various diseases (cancer, atherosclerosis, Alzheimer's disease, etc.). We studied the effects of ROS on the cyan fluorescent protein (CFP) *in vitro,* as this fluorescent protein is currently one of the most widely used in protein interaction studies. We studied the fluorescence and absorption changes of recombinant CFP protein using γ-radiolysis for ROS production. γ-radiolysis ROS production allowed us to have an exact control over the radical concentrations delivered unto the protein samples. The radicals used in this study were OH°, O_2^{-} or a mixture of OH° and O_2^{-}. We also determined the chemical modifications that take place upon ROS induced protein oxidation by mass spectrometry. We show that the targets of oxidation are one tyrosine and four methionine residues located on the protein surface and that the chromophore is not likely modified through these oxidation processes.

341-Pos Board B220

Thermodynamic Intermediates of the Alkaline III→IV Transition in Ferricytochrome c Probed by 695 nm Charge Transfer Band

Daniel Verbaro[1], Andrew Hagarman[1], Carmichael Wallace[2], Reinhard Schweitzer-Stenner[1].
[1]Drexel University, Philadelphia, PA, USA, [2]Dalhousie University, Halifax, NS, Canada.

The 695 nm band in the spectrum of the native state (III) of ferricytochrome c has recently been shown to be composed of different sub-bands which reflect different conformational substates (CS) of the functional pivotal Fe-M80 linkage. In order to explore the influence of the alkaline III→IV transition on this CSs we measured and analyzed the absorption and CD profile of this band as a function of pH between pH 7 and 10 at high (50mM) and low anion concentration for horse heart (hh) cytochrome c. Additional measurements on yeast cytochrome c were performed at low anion concentrations. The titration curves of the two dominating sub-bands are clearly biphasic at low anion concentrations and reflect effective pK-values of 8.5 and 9.65. On the contrary, the titrations curves obtained at high anion concentrations are monophasic; the effective pK being 9.23. The thermodynamic parameters (i.e. pK and the Hill coefficient as a measure of cooperativity) are slightly different for the two CSs. We fitted the data obtained at low anion concentration with a model, which assigns the two effective pK-values to two different alkaline states IV1 and IV2, in which M80 is replaced by K73 and K79, respectively. This model did not reproduce our data well in contrast to an alternative model which assumes only one species with two protonation sites. This suggests that the state populated upon the pK= 8.5 protonation can be interpreted as a thermodynamic intermediate of the III→IV transition. This notion is consistent with our observation, that the 695 nm titration curves of the y-cytochrome c mutants K79R and K73V are still mostly biphasic at low ionic strength.

342-Pos Board B221

X-ray Footprinting at Beamline X28C: A National Resource for Studying Macromolecular Structure and Dynamics

Rhijuta D'Mello, Sayan Gupta, Jen Bohon, Donald Abel, John Toomey, Michael Sullivan, Mark R. Chance.
Case Western Reserve University, Upton, NY, USA.

X-ray footprinting employs intense X-rays produced by synchrotron radiation to generate hydroxyl radicals in solution on microseconds-milliseconds timescales. These hydroxyls radicals undergo stable reaction with solvent accessible sites of macromolecule and produce covalent modifications, which are appropriate to probing macromolecule dynamics under physiological condition. For nucleic acids, one analyzes the pattern of fragments after X-ray exposure by gel electrophoresis; the protected sections that are not cleaved yield a ''footprint''. For proteins, the exposed samples are digested with proteases and analyzed by liquid chromatography- and tandem-mass spectrometry to determine the extent and sites of modification. The data provide detailed structural information to map tertiary contacts of macromolecular interactions, which can subsequently be used as constraints for molecular modeling to generate high-resolution

structures. This method is unique in providing ''local'' structural information in solution for gaining insight into dynamic processes involving, large RNA-protein and protein-protein assemblies on biologically relevant timescales. The method also can uniquely probe the ''local'' structure of large complexes poised at equilibrium for functional states of interest, and has been extended to *in vivo* studies.

Beamline X28C is located at the National Synchrotron Light Source of Brookhaven National Laboratory. An expanding set of user groups utilize this national resource funded by the National Institute of Biomedical Imaging and Bioengineering of the National Institutes of Health. The facility is operated by the Center for Synchrotron Biosciences and the Center for Proteomics and Bioinformatics of Case Western Reserve University. The facility supports both onsite and offsite user access. Beam time is allocated online through peer reviewed user proposal system. Examples of recent research projects are provided.

343-Pos Board B222

Expression and Purification of the Myxoma Virus Leukemia Associated Protein Zinc Finger Domain

Bryan G. Hahn[1], Dominic Esposito[2], Dana C. Lawrence[1].
[1]Hood College, Frederick, MD, USA, [2]SAIC-Frederick, Frederick, MD, USA.

Myxoma Virus Leukemia Associated Protein (MV-LAP) is a protein encoded by Myxoma virus, a poxvirus responsible for the lethal disease, myxomatosis in the European Rabbit. MV-LAP has developed a ''stealth'' mechanism to evade the host immune system by reducing the expression of major histocompatibility complex (MHC)-1 molecules, responsible for identifying self vs. non-self antigens. In order to help understand this stealth mechanism, the N-terminal domain (NTD; 94 residues) of MV-LAP will be characterized structurally using NMR. The current project builds upon the purification of the MV-LAP-Maltose Binding Protein fusion protein system and the purification of MV-LAP NTD. Purification of the fusion protein occurred via the use of a Co^{2+} Immobilized Metal ion Affinity Chromatography (IMAC) column. Several buffer systems allow for the purification of a soluble fusion protein. In addition, several buffer systems were evaluated for the use in the purification of MV-LAP NTD. The purification of a soluble form of MV-LAP NTD and the preparation of a sample for NMR analysis is currently underway.

344-Pos Board B223

Expression and Purification of Zinc Finger Antiviral Protein

Christina M. Zimmerman[1], Dominic Esposito[2], Dana C. Lawrence[1].
[1]Hood College, Frederick, MD, USA, [2]SAIC-Frederick, Frederick, MD, USA.

Ever since the discovery of viruses so many years ago there have been researchers of many different fields racing to find the perfect inhibitor. Any and all discoveries of viral resistance have been taken into a spotlight to discover the mechanisms. Zinc Finger Antiviral Protein (ZAP) is found in the kidney and liver cells of *Rattus norvegicus*; this protein makes these cells more resistant to viral infection. Gao et al concluded that ZAP facilitates inhibition of the antiviral gene expression, one of the major propagation steps (rather than inhibition of infection ZAP affects viral expression) by binding viral mRNA. Since then ZAP has been shown to increase resistance against Moloney Murine Leukemia virus, Sindbis virus, Ebola virus, and Marburg virus. Activity of ZAP containing four CCCH zinc fingers seems to be dependent on the integrity of the second and fourth CCCH zinc fingers. With HIV in mind, which is also a retrovirus, we have concluded that ZAP will have profound and influential implications.

Our goal is to determine the structure of the zinc-binding domain of ZAP using Nuclear Magnetic Resonance. Zap was expressed as a fusion protein in *E. coli* with several different cleavage conditions and purified using Immobilized Metal Ion Affinity Chromatography (IMAC) were screened and found unsuccessful in that the cleaved ZAP was insoluble. However, we are currently working on the smaller ZAP proteins that only contain two zinc fingers; their constructs show promising results in terms of solubility after cleavage.

345-Pos Board B224

Troponin T Deletion 96 Related to Restrictive Cardiomyopathy Ablates the Effects of Cardiac Troponin I PKA Pseudo-Phosphorylation on Ca^{2+} Sensitivity of Force Development

Michelle S. Parvatiyar, Jose R. Pinto, Jingsheng Liang, Michelle A. Jones, James D. Potter.
University of Miami, Miller School of Medicine, Miami, FL, USA.

The human cardiac TnT deletion 96 (HcTnT3-ΔE96) has been linked to Restrictive Cardiomyopathy and causes a dramatic increase in Ca^{2+} sensitivity of force development (J Biol Chem 283(4):2156-66). Here, we present further biochemical and functional studies to assess whether there are additional factors contributing to the severity of the phenotype. To determine whether the RCM mutation interferes with the cTnI-PKA phosphorylation signal, that decreases Ca^{2+} sensitivity of the myofilament upon β-adrenergic stimulation, we utilized a cTnI phosphorylation mimetic. The Ca^{2+} sensitivity of force development was evaluated in porcine cardiac skinned fibers using cTnT displacement (HcTnT3-WT or HcTnT3-ΔE96) followed by reconstitution with the binary complex containing pseudo-phosphorylated cTnI (where serines 23, 24 were replaced with aspartic acid - $cTnI_{SS/DD}$.cTnC) or the non-phosphorylatable control cTnI (where serines 23, 24 were mutated to alanine - $cTnI_{SS/AA}$.cTnC). Fibers displaced with HcTnT3-WT and reconstituted with $cTnI_{SS/DD}$.cTnC showed a decrease in the Ca^{2+} sensitivity compared to the control reconstituted with $cTnI_{SS/AA}$.cTnC. In contrast, fibers displaced with HcTnT3-ΔE96 and reconstituted with $cTnI_{SS/DD}$.cTnC or $cTnI_{SS/AA}$.cTnC showed similar Ca^{2+} sensitivities. These results indicate that the mutation may ablate the effects of cTnI PKA phosphorylation. Additionally, Circular dichroism (CD) studies using 0.5M NaF showed a decreased α-helical content of HCTnT3-ΔE96 compared to HCTnT3-WT. CD thermal denaturation measuring the α-helical content at 222 nm revealed that the mutant unfolded earlier and at a drastically reduced T_m compared to WT. Furthermore, Troponin complexes containing cTnC-IAANS labeled at both Cys 35 and 84 with HcTnT3-D96 did not show alterations in the apparent Ca^{2+} affinity of the cTnC low affinity site II compared to troponin complex containing HcTnT3-WT. Work supported by NIH HL-042325 (J.D.P.) and Postdoctoral Fellowship AHA 0825368E (J.R.P.).

346-Pos Board B225

Structural Comparison Of A Diabetes Drug Target, Mitoneet, A 2Fe-2S Cluster Protein To Its More Stable Mutant, H87C

Andrea R. Conlan[1], Herbert L. Axelrod[2], Aina E. Cohen[2], Edward C. Abresch[1], Rachel Nechushtai[3], Mark L. Paddock[1], Patricia A. Jennings[1].
[1]UCSD, La Jolla, CA, USA, [2]Stanford Synchrotron Radiation Laboratory, Menlo Park, CA, USA, [3]The Hebrew University of Jerusalem, Jerusalem, Israel.

MitoNEET, a recently discovered 2Fe-2S containing outer mitochondrial protein (1), was identified as a binding target for pioglitazone, an insulin-sensitizing drug of the thiazolidinedione class used in the treatment of type 2 diabetes (2). MitoNEET possesses a unique dimeric structure, with a new fold (3). The pH sensitive lability of the 2Fe-2S cluster was attributed to protonation of the conserved solvent accessible His87 (Figure). Its replacement with Cys increased the stability of the cluster ~10-fold (1). The crystal structure of the H87C mutant (1.8Å, Rfactor = 18%) shows that the Sγ of Cys87 remains at a similar position to the Nδ of His87 in the native (Figure). The only other change was a reorientation of Lys55. Thus, the increased stability of the HC87 mutant is attributed to the specific change in the ligation of the 2Fe-2S cluster, not a more global conformational change.

(1) Wiley et al. (2007) J Biol Chem. 282, 23745-23749.
(2) Colca et al. (2004) Am J Physiol Endocrinol Metab 286, E252-E260.
(3) Paddock et al. (2007) Proc Natl. Acad. Sci USA 104, 14342-14347.
*Supported by NIH (GM41637, GM54038 and DK5441).

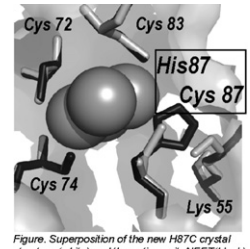

Figure. Superposition of the new H87C crystal structure (white) and the native mitoNEET(black) showing the 2Fe-2S cluster (spheres), a semitransparent view of the protein and its surface and specific amino acids (as labeled) that interact with the cluster.

347-Pos Board B226

Crystallographic Structure And Structural Stability Of Vertebrate Digestive Lysozyme

Yasuhiro Nonaka[1], Daisuke Akieda[1], Nobuhisa Watanabe[2], Masakatsu Kamiya[1], Tomoyasu Aizawa[1], Makoto Demura[1], Keiichi Kawano[1].
[1]Hokkaido University, Sapporo, Japan, [2]Nagoya University, Nagoya, Japan.

C-type lysozyme catalyzes the hydrolysis of peptidoglycan of bacterial cell wall. Most of C-type lysozymes express to protect body against bacterial infection. However, ruminants and some leaf-eating animals have evolved their lysozyme as digestive enzyme. They recruit bacteria which ferment cellulose in the foregut, and digest the bacteria by lysozyme in the true stomach to obtain nutrient. Digestive lysozyme has acquired some properties, such as low optimal pH, and resistance to protease and acid hydrolysis. The structural basis for these properties still remains unclear. In this investigation, we have obtained the crystallographic structure of bovine stomach lysozyme (BSL). This is the first report on the structure of vertebrate digestive lysozyme. We have carried out the denaturant-unfolding experiment and revealed that BSL has high structural stability at acidic pH compared to non-digestive (hen egg-white) lysozyme. The structural stability in acidic solution would be related to the pepsin resistance